Helium isotopes in ferromanganese crusts from the central Pacific Ocean

S. Basu [a,*], F.M. Stuart [a], V. Klemm [b], G. Korschinek [c], K. Knie [c], J.R. Hein [d]

[a] *Isotope Geosciences Unit, Scottish Universities Environmental Research Centre, East Kilbride G75 0QF, UK*
[b] *Institute for Isotope Geochemistry and Mineral Resources, Department of Earth Sciences, ETH-Zurich, ETH Zentrum, Sonneggstrasse 5, CH+8092 Zurich, Switzerland*
[c] *Technische Universität München, Fakultät für Physik, James-Franck-Straße 1, D-85747 Garching, Germany*
[d] *U.S. Geological Survey, 345 Middlefield Road, MS-999, Menlo Park, CA 94025, USA*

Abstract

Helium isotopes have been measured in samples of two ferromanganese crusts (VA13/2 and CD29-2) from the central Pacific Ocean. With the exception of the deepest part of crust CD29-2 the data can be explained by a mixture of implanted solar- and galactic cosmic ray-produced (GCR) He, in extraterrestrial grains, and radiogenic He in wind-borne continental dust grains. ^{4}He concentrations are invariant and require retention of less than 12% of the *in situ* He produced since crust formation. Loss has occurred by recoil and diffusion. High ^{4}He in CD29-2 samples older than 42 Ma are correlated with phosphatization and can be explained by retention of up to 12% of the *in situ*-produced ^{4}He. ^{3}He/^{4}He of VA13/2 samples varies from 18.5 to 1852 R_a due almost entirely to variation in the extraterrestrial He contribution. The highest ^{3}He/^{4}He is comparable to the highest values measured in interplanetary dust particles (IDPs) and micrometeorites (MMs). Helium concentrations are orders of magnitude lower than in oceanic sediments reflecting the low trapping efficiency for in-falling terrestrial and extraterrestrial grains of Fe-Mn crusts. The extraterrestrial ^{3}He concentration of the crusts rules out whole, undegassed 4–40 μm diameter IDPs as the host. Instead it requires that the extraterrestrial He inventory is carried by numerous particles with significantly lower He concentrations, and occasional high concentration GCR-He-bearing particles.

1. Introduction

Ferromanganese (Fe-Mn) crusts form on ocean-floor rock substrates as hydrogenous precipitates and preserve long-term records of the chemical composition of seawater. In particular, the isotopic compositions of Pb, Nd, Hf, and Os in Fe-Mn crusts record changes in the delivery of terrestrial material to the oceans that allow constraints to be placed on ocean circulation and climate over the last few tens of million years (e.g. Ling et al., 1997; Burton et al., 1999; Frank et al., 1999; Frank, 2002; Van de Flierdt et al., 2003). The reconstruction of past changes in seawater composition is predicated on accurate chronologies for the growth of the crusts that are provided by Co concentrations (e.g. Halbach et al., 1983), ^{10}Be (e.g. Segl et al., 1984; Ling et al., 1997), and Os isotopes (Klemm et al., 2005).

Helium isotopes in oceanic sediments provide useful information on the flux of terrestrial and extraterrestrial debris to the sea floor over geological time. ^{4}He is supplied by detrital minerals and is a proxy for the delivery of continental material to the deep oceans in the form of wind-blown debris (e.g. Patterson et al., 1999). In contrast, ^{3}He provides a record of the accumulation of in-falling extraterrestrial dust-sized particles that can be used to identify major cometary shower and asteroidal break-up events, associated with increasing dustiness in the inner solar system (e.g. Farley, 1995). ^{3}He can also be used to determine sedimentation rates beyond the range possible using conventional radiometric techniques (e.g. Marcantonio et al., 1996).

The potential to use He isotopes in Fe-Mn crusts to trace long-term fluctuations in the delivery of extraterrestrial and

---

* Corresponding author. Fax: +44 0 1355 229898.
  E-mail address: s.basu@suerc.gla.ac.uk (S. Basu).

terrestrial material to the oceans remains largely untested. Early efforts demonstrated that extraterrestrial He signatures are trapped and preserved in the outer layers of Fe-Mn nodules (Sano et al., 1985). Here, we present the first systematic He isotope study of dated layers in Fe-Mn crusts in an attempt to determine the source of terrestrial and extraterrestrial He in the oceans as well as assessing the prospects for using the ingrowth of radiogenic He as a chronometer of crust growth.

2. Samples and techniques

Helium isotopes have been determined in samples from two Fe-Mn crusts (VA13/2 and CD29-2) from the central Pacific Ocean. These crusts are ideally suited for the search for extraterrestrial noble gases as they have low growth rates, they are from a deep ocean basin where the delivery rate of terrestrial sediment is low, and they have been subjected to detailed mineralogical, chronometric, geochemical and isotopic investigation.

CD29-2 (16°42.4′N, 168°14.2′W) was dredged from a water depth of 2.3 km on a seamount on the Karin Ridge south of the Hawaiian Ridge during cruise F7-86-HW (Hein et al., 1990). It is 110 mm thick and is dominantly composed of vernadite (δ-MnO_2) with approximately 1% detrital quartz and plagioclase (Hein et al., 1990; Frank et al., 1999). From the variation in $^{10}Be/^9Be$ with crust depth, the upper 21 mm is calculated to have accreted at an average rate of 2.1 mm/Myr (Ling et al., 1997). Extrapolating this growth rate yields an age of 50 Ma for the base of the crust. However, new Os isotope chronology indicates that growth started prior to 70 Ma with major hiatuses at 44–46, 31–34 and 15–28 Ma (Klemm et al., 2005). Secondary phosphatization of the primary crust mineralogy produced 7–10% carbonate fluorapatite (CFA) below 52 mm (Hein et al., 1990, 2000). Although the phosphatization resulted in element redistribution, it appears not to have affected the Nd, Pb, or Os isotopic records (Christensen et al., 1997; Frank et al., 1999; Klemm et al., 2005). Helium isotopes were determined in 31 sub-samples of CD29-2. Samples were taken from 4.5 to 105 mm depth, corresponding to an age range of 2–72 Ma (Klemm et al., 2005). Sample names in Table 1 reflect the depth from the outermost surface of the crust, i.e. CD29-2(4-5) is from 4 to 5 mm. Samples with suffix B were drilled from the base of the crust and the identification numbers reflect distance from the bottom of the crust, e.g. CD29-2(2-3B) is from interval 2 to 3 mm above the base.

Crust VA13/2 (9°18′N, 168°146.03′W) was collected from a water depth of 4.8 km from an abyssal hill during cruise Valdiva in the central Pacific Ocean (Friedrich and Schmitz-Wiechowsky, 1980). It is smooth and gently rounded on the surface with numerous internal mm-sized microlayers (Friedrich and Schmitz-Wiechowsky, 1980). It is largely composed of vernadite and amorphous Fe oxyhydroxide, with minor detrital plagioclase and quartz for the upper 105 mm (Von Stackelberg et al., 1984). Below a

Table 1
Total ^{4}He, ^{3}He/^{4}He and calculated extraterrestrial ^{3}He (^{3}He$_{et}$) concentrations in Fe-Mn crusts VA13/2 and CD29-2 from the central Pacific Ocean

Sample	Age (Ma)[a]	^{4}He (10^{12} atoms/g)	^{3}He/^{4}He (R/R_a)[c]	^{3}He$_{et}$ (10^7 atoms/g)
VA13/2				
VA13/2(0-1)a[b]	0.4	1.74 ± 0.03	237.7 ± 5.8	57.6 ± 0.9
VA13/2(0-1)b[b]		1.33 ± 0.02	1852 ± 31	345 ± 3
VA13/2(0-1)c[b]		1.16 ± 0.02	312 ± 12	50.2 ± 1.8
VA13/2(0-1)d[b]		1.21 ± 0.03	983 ± 26	165 ± 2
VA13/2(1-2)	0.8	1.72 ± 0.04	106.4 ± 4.1	25.5 ± 0.8
VA13/2(2-3)	1.2	1.40 ± 0.01	84.0 ± 4.0	16.0 ± 0.8
VA13/2(3-4)	1.6	0.88 ± 0.03	110.6 ± 7.2	13.6 ± 1.4
VA13/2(4-5)	2.0	1.02 ± 0.04	66.7 ± 3.1	9.4 ± 0.3
VA13/2(5-6)a[b]	2.4	1.03 ± 0.01	297.5 ± 7.2	42.8 ± 1.0
VA13/2(5-6)b[b]		0.58 ± 0.02	26.2 ± 4.2	2.1 ± 0.3
VA13/2(5-6)c[b]		0.53 ± 0.01	29.6 ± 2.6	2.2 ± 0.2
VA13/2(5-6)d[b]		0.48 ± 0.01	32.6 ± 3.4	2.2 ± 0.2
VA13/2(6-7)	2.8	1.07 ± 0.01	251.8 ± 8.1	37.3 ± 1.1
VA13/2(7-8)	3.2	1.03 ± 0.02	159.6 ± 5.1	22.8 ± 0.6
VA13/2(8-9)	3.6	1.10 ± 0.02	240 ± 11	36.8 ± 1.5
VA13/2(9-10)	4	1.23 ± 0.03	18.5 ± 2.2	3.2 ± 0.4
CD29-2				
CD29-2(4-5)	2	1.11 ± 0.01	14.9 ± 0.9	2.3 ± 0.1
CD29-2(10-11)	5	0.68 ± 0.01	14.6 ± 1.3	1.38 ± 0.12
CD29-2(12-13)	6	0.40 ± 0.01	23.9 ± 1.8	1.32 ± 0.10
CD29-2(15-16)	7	2.76 ± 0.01	17.9 ± 0.7	6.8 ± 0.3
CD29-2(17-18)	8	1.49 ± 0.01	9.2 ± 1.0	1.9 ± 0.2
CD29-2(19-20)	9	1.08 ± 0.01	8.3 ± 0.9	1.23 ± 0.13
CD29-2(21-22)	10	1.24 ± 0.01	8.4 ± 0.6	1.44 ± 0.10
CD29-2(23-24)	11	1.06 ± 0.01	9.7 ± 1.4	1.42 ± 0.20
CD29-2(25-26)	12	3.39 ± 0.01	4.0 ± 0.3	1.9 ± 0.1
CD29-2(27-28)	13	1.90 ± 0.01	10.3 ± 0.9	2.7 ± 0.1
CD29-2(29-30)	14	1.60 ± 0.01	5.3 ± 0.4	1.18 ± 0.09
CD29-2(31-32)	30	0.81 ± 0.01	7.5 ± 1.1	0.85 ± 0.12
CD29-2(43-44)	39	2.94 ± 0.01	6.2 ± 0.5	2.5 ± 0.2
CD29-2(45-46)	40	6.19 ± 0.01	1.4 ± 0.2	1.14 ± 0.19
CD29-2(47-48)	41	2.59 ± 0.01	2.9 ± 0.3	1.02 ± 0.10
CD29-2(49-50)	42	6.68 ± 0.01	0.87 ± 0.11	0.76 ± 0.09
CD29-2(51-52)	43	29.60 ± 0.03	0.21 ± 0.03	0.66 ± 0.07
CD29-2(53-54)	47	46.34 ± 0.03	0.18 ± 0.02	0.84 ± 0.05
CD29-2(55-56)	48	48.63 ± 0.02	0.14 ± 0.01	0.61 ± 0.05
CD29-2(57-58)	49	132.4 ± 0.1	0.064 ± 0.004	0.24 ± 0.02
CD29-2(61-62)	51	139.7 ± 0.2	0.038 ± 0.002	n.c.
CD29-2(67-68)	54	83.54 ± 0.03	0.12 ± 0.02	0.78 ± 0.09
CD29-2(71-72)	56	73.13 ± 0.03	0.15 ± 0.01	0.99 ± 0.09
CD29-2(18-19B)	63	85.44 ± 0.03	0.033 ± 0.011	n.c.
CD29-2(16-17B)	64	57.54 ± 0.04	0.062 ± 0.016	0.09 ± 0.02
CD29-2(14-15B)	65	2.04 ± 0.01	0.046 ± 0.008	n.c.
CD29-2(12-13B)	66	80.13 ± 0.03	n.m.	
CD29-2(10-11B)	67	79.77 ± 0.03	0.034 ± 0.006	0.38 ± 0.02
CD29-2(6-7B)	69	0.45 ± 0.04	3.4 ± 0.9	0.21 ± 0.05
CD29-2(2-3B)	71	68.4 ± 0.1	n.m.	
CD29-2(0-1B)	72	117.0 ± 0.2	n.m.	

n.m., not measurable, ^{3}He below detection level.
n.c, not calculable, ^{3}He/^{4}He is lower than assumed crustal value of 0.05 R_a.
[a] Age of VA13/2 is obtained from an average growth rate of 2.5 mm/ Myr (Knie et al., 2004). The age of CD29-2 samples are from Klemm et al. (2005).
[b] Denotes sub-samples.
[c] ^{3}He/^{4}He, R, is normalised to the atmospheric ^{3}He/^{4}He of 1.4×10^{-6} (R_a).

depth of 105 mm—corresponding to approximately 19 Ma—the crust is composed of almost pure goethite (Frank et al., 1999). Based on $^{10}Be/^9Be$, the outer 16 mm

is estimated to have grown at a rate of 2.7 mm/Myr since 6 Ma (Segl et al., 1984). From combined $^{10}Be/^9Be$ age and Co concentrations, the crust is estimated to be 26.5 Ma at its base (Frank et al., 1999). The bulk chemical composition of the crust is largely derived from seawater and not leached from the basaltic substrate (Hein and Morgan, 1999), although the older section has a Pb isotope composition indicative of a significant hydrothermal component (Frank et al., 1999). A peak in the ^{60}Fe record at 2.8 Ma is attributed to the incorporation of supernova ejecta by the crust (Knie et al., 2004). Sample names refer to the depth in the crust, e.g. VA13/2(0-1) represents the top 0–1 mm. Helium isotopes have been analysed in samples from the outermost 10 mm of the crust (Table 1). Four sub-samples of VA13/2(0-1) and VA13/2(5-6) were analysed in order to assess the consistency of the He isotope record of any individual sample.

All samples were cleaned in acetone then rinsed in distilled water. Between 5 and 10 mg of each sample from VA13/2, and 10 to 20 mg from CD29-2, were weighed into Al foil packets and approximately 20 were loaded into branches of a Monax glass tree and evacuated to 10^{-8} mbar. Each sample was dropped in turn through an all-metal gate valve into a conventional double-walled resistance furnace and heated at 900 °C for 20 min. Water was absorbed onto liquid nitrogen-cooled metal adjacent to the furnace during gas extraction prior to purification by exposure to hot ZrAl getters. The residual gases were equilibrated with liquid nitrogen-cooled charcoal for removal of heavy noble gases prior to admission to the mass spectrometer. He and Ne abundances and He isotopic compositions were determined using a MAP 215-50 magnetic sector mass spectrometer equipped with a Faraday cup for ^4He and pulse-counting electron multiplier operated at 3 kV for ^3He. A liquid nitrogen-cooled charcoal finger and a getter in the mass spectrometer volume were used to minimise the partial pressure of interfering species during analysis. A resolving power of 600 was adequate for the separation of $^3He^+$ and HD^+. Gas extraction at 1400 °C was routinely performed, and in all cases He was at blank levels indicating complete extraction of He at 900 °C. Helium blanks at 900 and 1400 °C were indistinguishable. The ^4He blank averaged 2.9×10^8 atoms and never contributed more than 1% to each sample. The ^3He blank averaged approximately 7000 atoms and contributed less than 5% to all VA13/2 and CD29-2 samples where ^3He data are reported, except for samples CD29-2 (6-7B), (10-11B), (16-17B) and (18-19B) where blanks ranged from 7% to 13%.

3. Results

The ^4He concentrations and $^3He/^4He$ normalised to the air ratio (R_a: 1.39×10^{-6}) are listed in Table 1. The VA13/2 samples have a narrow range of ^4He, from 0.48 to 1.74×10^{12} atoms/g. The three youngest samples (VA13/2 (0-1), (1-2), and (2-3)) have the highest He concentrations,

while VA13/2(5-6) has the lowest. ^3He concentrations are significantly more variable, ranging from 2.1 to 345×10^7 atoms/g. $^3He/^4He$ ranges from 18.5 ± 2.2 R_a (VA13/2(9-10)) to 1852 ± 31 R_a (VA13/2(0-1)b), with values in excess of 200 R_a occurring in 7 of the 16 analyses. The highest $^3He/^4He$ is comparable to the highest values measured in stratospheric interplanetary dust particles (IDPs) (2221 ± 68 R_a; Pepin et al., 2000) and micrometeorites (MMs) (1543 ± 357 R_a; Marty et al., 2005). The VA13/2 data form a linear array in $^4He/^3He$ vs. $1/^3He$ space that is consistent with two-component mixing (Fig. 1).

^4He concentrations in CD29-2 range from 0.40×10^{12} to 139.7×10^{12} atoms/g (Table 1; Fig. 2a). For samples down to 50 mm (i.e. 2–42 Ma) ^4He concentrations are similar to those of VA13/2; $0.40-6.68 \times 10^{12}$ atoms/g. Between layers at 51/52 mm and 60 mm ^4He concentrations increase to approximately 1×10^{14} atoms/g, and remain at that level to the base of the crust. Down to 47/48 mm ^3He concentrations are relatively uniform ($0.85-6.8 \times 10^7$ atoms/g) (Fig. 2b). At depths greater than 48 mm ^3He concentrations are significantly lower, with three samples yielding no measurable ^3He above detection limit (ca.10^5 atoms). Consequently $^3He/^4He$ shows a strong co-variation with age (Fig. 2c). The 15 samples from the upper 46 mm range from 1.4 ± 0.2 R_a (45–46 mm) to 23.9 ± 1.8 R_a (12–13 mm). With the exception of CD29-2(6-7B) (3.4 R_a), the samples from deeper than 50 mm never exceed 0.2 R_a (Table 1). The samples from 0 to 47 mm have $^3He/^4He$ that are significantly lower than crust VA13/2 data and plot at the high $^4He/^3He$ end of the trend in $^4He/^3He$ vs. $1/^3He$ space defined by VA13/2 samples (Fig. 1). The ^3He concentrations and $^3He/^4He$ of the crusts are generally higher than Fe-Mn nodules from the Pacific Ocean (Sano et al., 1985).

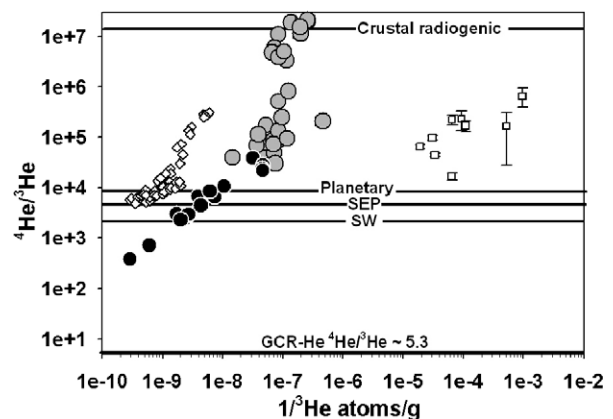Fig. 1. Plot of $1/^3He$ vs. $^4He/^3He$ for crust VA13/2 (black circles) and CD29-2 (grey circles), indicating two component mixing between extraterrestrial and crustal components. Samples with very high $^4He/^3He$ do not plot on the trend and may be related to phosphatization. Fe-Mn nodules (white circles; Sano et al., 1985) do not plot on the same array as the crusts due to higher growth rates and/or higher crustal He contributions. Red clays from sediment core GPC-3 (white dotted circles; Farley, 1995) show a slightly different trend that may be attributed to different accumulation rates.
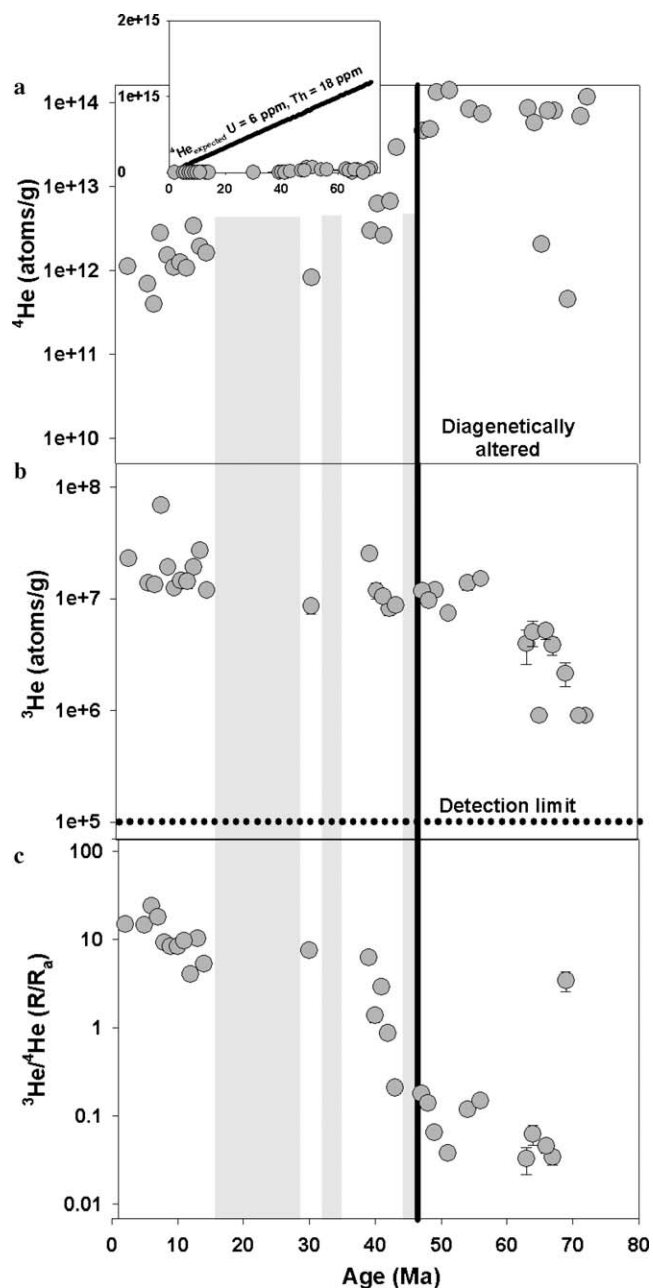
Fig. 2. (a) Plot of ^{4}He vs. age for CD29-2 compared to the expected ^{4}He for average U and Th (6 and 18 ppm: Ling et al., 1997). The data require significant loss of *in situ* ^{4}He from the samples. The high ^{4}He in samples precipitated prior to 42 Ma may be due to better retention of *in situ* ^{4}He in phosphatized crust, marked by the black bold line. Hiatuses are marked by grey shades. (b) Plot of ^{3}He vs. age for CD29-2 indicates a significant decrease in ^{3}He in the pre-56 Ma samples. This may result from the loss of ^{3}He from the extraterrestrial grains by breakdown during phosphatization process. (c) Plot of ^{3}He/^{4}He vs. age for CD29-2.

4. Discussion

4.1. Source of helium in ferromanganese crusts

Extensive studies of deep ocean pelagic sediments have demonstrated that helium is largely a mixture of extraterrestrial He (^{3}He/^{4}He = 290 R_a) similar to solar wind and bulk lunar fines, in interplanetary dust particles (IDP),

and radiogenic He (ca. 0.05 R_a) in detrital minerals delivered as aeolian dust (e.g. Ozima et al., 1984; Takayanagi and Ozima, 1987; Patterson et al., 1999). Although this is the simplest interpretation for the bulk of the Fe-Mn crust He isotope data, there are several other potential sources of helium (Farley, 2001). It is pertinent here to address the possible alternative sources of He in Fe-Mn crusts.

(i) Mantle He is emitted in hydrothermal fluids at mid-ocean ridges, and trapping of these fluids by growing crusts would add He with ^{3}He/^{4}He of approximately 8 R_a (Lupton et al., 1980). However, away from mid-ocean ridges ^{3}He concentrations rapidly approach seawater values and incorporation of excesses into growing crusts is not likely to be significant. Incorporation of hydrothermal sulfide minerals, although unlikely, would also provide a source of mantle He. Similarly mid-ocean ridge hydrothermal sulfides have He concentrations that are orders of magnitude lower than recorded by the Fe-Mn crusts (Turner and Stuart, 1992; Stuart et al., 1994) and are also unlikely to be a significant contributor. The average Fe/Mn of VA13/2 and CD29-2 are 1.0 and 0.7, respectively (Friedrich and Schmitz-Wiechowsky, 1980; Hein et al., 1990). These are lower than the values generally observed for mixed hydrogenetic and hydrothermal crusts (1.3–3) (Hein et al., 1990), and provide no evidence for a significant hydrothermal contribution to the crusts.

(ii) Decay of U and Th incorporated into the crust during formation produces *in situ* ^{4}He. In crust CD29-2, U concentrations range from 2.1 to 10.2 ppm (Ling et al., 1997). For [U] = 6 ppm and Th/U = 3, ingrowth of ^{4}He should dominate the measured ^{4}He in all samples within less than a few Myr (Fig. 2a, inset). The rather constant ^{4}He concentration of all samples from less than 46 Ma, and the absence of a relationship between ^{4}He concentration and sample age (Fig. 2a), implies that *in situ* ^{4}He is not quantitatively retained by the crust minerals.

Fe-Mn crust minerals (δ-MnO$_2$, Fe-oxyhydroxides and CFA) have an average grain size of less than 1 µm as inferred from their specific surface area of 200–400 m^2/g (Hein et al., 2000). *In situ* ^{4}He originates as α-particles that recoil 15–25 µm in minerals after production by radioactive decay of U, Th, and their daughter products (Farley et al., 1996). Consequently, no ^{4}He atoms come to rest in the mineral grain in which they were produced. All the *in situ* He that stops in pore space and grain boundaries is lost to seawater. The high porosity of Fe-Mn crusts (40–75%; Hein et al., 1985; Yamazaki et al., 1990) will result in recoil loss of a significant proportion of the He at the time of production. The longer α-recoil distance in water compared to minerals results in a lower proportion stopping in pore space than that predicted simply from porosity, but will result in the loss of 10's % of the *in situ* ^{4}He. However, the almost complete absence of *in situ* ^{4}He in the majority of crust samples implies that even the He that is implanted into crust minerals is lost instantaneously. It is well established that He is completely lost from many minerals by diffusion at surface temperatures (e.g. Trull et al., 1989).

The retention of 10% of the *in situ* He by 1 μm minerals for less than 100 kyr at seafloor temperatures (which can be assumed from the near absence of radiogenic He in the youngest samples) requires diffusion rates of 1–5×10^{-22} cm²/s. Helium diffusion rates have not been determined for the primary crust minerals; carbonate fluorapatite and vernadite. The diffusion rate of He in minerals closest in composition to those of the crust (apatite 2×10^{-25} cm²/s; Farley, 2000), goethite (6×10^{-30} cm²/s; Shuster et al., 2005) and hematite (3×10^{-31} cm²/s; Wernicke and Lippolt, 1994)) at 2 °C, is too slow to account for the absence of radiogenic He. The role of diffusive loss from crust minerals awaits He diffusion rate studies but it is pertinent to note that pelagic clay radiogenic ^{4}He concentrations are two orders of magnitude lower than predicted from closed-system ingrowth (Farley, 1995). The absence of *in situ* ^{4}He in the crusts means that the (U-Th)/He dating method, currently finding uses in many fields, is not a viable method of determining the age of Fe-Mn crusts.

(iii) Nucleogenic ^{3}He is generated via the (n, α) reaction on ^{6}Li, where the neutrons originate from (α, n) reactions on light elements. For a neutron flux of normal crustal rocks, an unfeasibly high Li content of 38% is necessary to produce the ^{3}He in VA13/2(0-1)b. The Li content of a similar crust (4.62 ppm) (Henderson and Burton, 1999) produces trivial ^{3}He that does not significantly contribute to the ^{3}He measured in the crusts.

The helium in the majority of the samples from both Fe-Mn crusts is therefore best explained as a simple binary mix of extraterrestrial and crustal radiogenic components (Fig. 1). Since the lower part of CD29-2 is phosphatized, these data need to be interpreted with caution. The narrow range of ^{4}He concentrations (0.40–6.68×10^{12} atoms/g) in VA13/2 and pristine CD29-2 samples implies a rather constant flux of crustal radiogenic He delivered in the detrital grains. Consequently the isotopic variation is due to variation in the extraterrestrial helium contribution. This is supported by 7- and 21-fold variations in ^{3}He concentrations between replicates of samples VA13/2(0-1) and (5-6), respectively (Table 1) despite the remarkable constancy of ^{4}He. The mixing trend is particularly well-defined for VA13/2 where ^{4}He concentrations (0.48–1.74×10^{12} atoms/g) vary by less than a factor of 4, while ^{3}He concentrations vary by more than 150 times (Table 1). The coherence of the mixing trend implies that crust growth rates have stayed relatively constant over time, as predicted from Be isotopes and the Co method (Segl et al., 1984; Christensen et al., 1997; Frank et al., 1999). The comparatively larger scatter in the CD29-2 data may reflect variation in crust growth rate and accumulation rate of the terrigenous dust component, as well as variation in the accumulation rate of extraterrestrial He-bearing grains.

4.2. Comparison with oceanic sediments

The concentration of extraterrestrial helium (^{3}He$_{et}$) in each crust sample is calculated from:

$$
\begin{aligned}
^3\text{He}_{et} = {}^3\text{He}_{measured} * [\{(^4\text{He}/^3\text{He})_{measured} \\
- (^4\text{He}/^3\text{He})_{rad}\}/\{(^4\text{He}/^3\text{He})_{et} \\
- (^4\text{He}/^3\text{He})_{rad}\}]
\end{aligned}
\tag{1}
$$

where $(^3\text{He}/^4\text{He})_{et} = 290\, R_a$ and the $(^3\text{He}/^4\text{He})_{rad} = 0.05\, R_a$ (Farley et al., 1998). For the samples where $(^3\text{He}/^4\text{He})_{measured}$ is greater than $290\, R_a$ all the measured ^{3}He can be considered to be extraterrestrial. Extraterrestrial ^{3}He concentrations range from 2.1 to 345×10^7 atoms/g (Table 1), and always comprise greater than 98% of the ^{3}He in VA13/2 samples. The ^{3}He$_{et}$ concentrations in un-phosphatized CD29-2 samples are lower by an order of magnitude, but still account for more than 98% of the measured ^{3}He (Table 1).

The mixing trend in Fig. 1 defines a maximum concentration of extraterrestrial ^{3}He of approximately 6×10^8 atoms/g in Fe-Mn crust VA13/2. Considering the growth rate of the crust and sample thickness of 1 mm, this represents the accumulation of extraterrestrial grains for approximately 500 kyr. For a crust density of 2 g/cm³ (Hein et al., 2000) this corresponds to a maximum extraterrestrial He flux of approximately 2×10^5 atoms/cm²/kyr. This is approximately 1% of the extraterrestrial ^{3}He flux measured from sediments from the central Pacific Ocean over a similar time period (1.4–2.7×10^7 atoms/cm²/kyr; Farley, 1995; Patterson and Farley, 1998; Winckler et al., 2004). This is highlighted in Fig. 1 by the pelagic clay from core GPC-3 from the central Pacific Ocean which has higher helium concentrations. The low apparent ^{3}He flux recorded by the crusts reflects the low trapping efficiency of extraterrestrial grains by Fe-Mn crusts that are likely a result of strong bottom currents at the site of crust deposition. This implies that crusts do not record the subtle variations in the delivery of extraterrestrial He recorded by pelagic oceanic sediments (e.g., Farley, 1995; Mukhopadhyay et al., 2001). Consequently it is unlikely that the noble gas isotopes will provide resolution to the problem of whether the ^{60}Fe peak in crust VA13/2 at 2.8 Ma records the deposition of supernova ejecta (Knie et al., 2004). The difference in extraterrestrial particle flux between pelagic clays and Mn nodules has previously been observed for Os (Esser and Turekian, 1988; Peucker-Ehrenbrink, 1996).

^{4}He concentrations in the crusts are significantly lower than in oceanic sediments. From the ^{4}He in VA13/2 (0.5–1.7×10^{12} atoms/g), the flux of He$_{rad}$ (3–9×10^8 atoms/cm²/kyr) is approximately 0.1% of the typical flux recorded by sediments from the central Pacific Ocean (2–8×10^{11} atoms/cm²/kyr; Patterson et al., 1999). Slowly accumulating Fe-Mn crusts are unlikely to record the subtle variations in the delivery of crustal He recorded by pelagic oceanic sediments (e.g. Patterson et al., 1999). That the crust He$_{rad}$ flux/He$_{et}$ flux ratio is approximately 10 times lower than for oceanic sediments reflects a lower trapping efficiency of detrital minerals by the ferromanganese crusts. Stokes Law calculations show that zircon grains typical of those present in aeolian dust (<5 μm) will settle 10 times more

slowly through seawater than a 20 µm, 2 g/cc extraterrestrial dust particle. The low radiogenic He content of the crusts may therefore reflect the preferential removal of detrital minerals in the water column by strong bottom currents above the site of crust growth compared to larger interplanetary dust and micrometeorites. The low radiogenic He content does not dilute the extraterrestrial He signature to the same extent as in pelagic clays, making the crusts a more useful source of information on the source of extraterrestrial material delivered to Earth.

4.3. Implications for the source of extraterrestrial ^{3}He to Earth

On the basis of ^{3}He concentrations and ^{3}He/^{4}He, VA13/2 has a markedly stronger extraterrestrial He signature than CD29-2 (Table 1) despite the close proximity of the two crusts and the similar accretion rates (Ling et al., 1997). Of the 16 samples of VA13/2, 10 have ^{3}He/^{4}He in excess of the value of trapped primordial He in meteorites (88 R_a; Busemann et al., 1998), ruling it out as the dominant source of He in extraterrestrial grains delivered to the deep oceans. Most VA13/2 samples have ^{3}He/^{4}He that are greater than the highest ratio measured in marine sediments (ca. 150 R_a: Farley, 1995). Two samples (0-1c and 5-6a) have ^{3}He/^{4}He that are in excess of the value measured in solar energetic particles (SEP-He = 150 R_a; Benkert et al., 1993) and are indistinguishable from the value of solar wind (SW-He = 290 R_a; Benkert et al., 1993) measured in bulk lunar fines (Geiss et al., 1972; Nier and Schlutter, 1990). However, two splits of sample VA13/2(0-1) (b and d) yield ^{3}He/^{4}He that are clearly higher than the solar wind value (1852 and 983 R_a, respectively) and require He produced by galactic cosmic rays (GCR-He ~120,000 R_a; Weiler, 2002). Although GCR-He has been detected in Antarctic micrometeorites (Stuart et al., 1999; Marty et al., 2005) and stratospheric IDPs (e.g. Nier and Schlutter, 1992), this is its first detection in seafloor sediments. While at least two He components are present in the extraterrestrial particles, the strongly linear trend described by the VA13/2 samples (Fig. 1) implies that the isotopic composition of extraterrestrial He in the crusts is rather uniform.

Despite the extensive use of helium isotopes in oceanic sediments as a tracer of extraterrestrial dust delivery to Earth, there is uncertainty regarding the carrier phase of extraterrestrial He in seafloor sediment. The prevailing view is that the extraterrestrial He originates as implanted solar wind in interplanetary dust particles that are small enough (<35 µm) to avoid melting during atmospheric entry (e.g. Ozima et al., 1984; Farley et al., 1997). Farley et al. (1997) calculated that the bulk of the He is delivered by 20 µm diameter IDPs, if it is mass-correlated, or 7 µm diameter particles if the He is dominantly a surface-implanted constituent. This is supported by the agreement between ^{3}He measurements in sediments and the expected statistical distribution for

the surface-correlated component (Farley et al., 1997), and the similarity of the release temperature of extraterrestrial He from IDPs (600 °C; Nier and Schlutter, 1992). Based on magnetic separations and chemical dissolution experiments, the carrier phases of extraterrestrial He have been proposed to be magnetite and a refractory silicate (Fukumoto et al., 1986; Amari and Ozima, 1988; Matsuda et al., 1990).

The extraterrestrial He in seafloor samples requires the preservation of the host mineral for tens of millions of years. The alteration and He loss from relatively robust micrometeorites during significantly shorter residence times in Antarctic ice (Osawa et al., 2003), and the likelihood of diffusive loss of implanted solar He in the outer, radiation-damaged few microns of each grain, tends to rule out the preservation of He in whole IDPs for sufficient time period. The majority of larger cosmic dust particles (micrometeorites; >30 µm diameter) are partially- or completely melted and assumed to be degassed of extraterrestrial volatiles during entry heating. However, partially melted micrometeorites recovered from Antarctic and Greenland ice often retain a significant component of the extraterrestrial He (Stuart et al., 1999; Osawa and Nagao, 2002; Osawa et al., 2003; Marty et al., 2005) and could make a significant contribution to the seafloor ^{3}He inventory if they survive weathering (Stuart et al., 1999). Lal and Jull (2005) calculated that a significant contribution of the GCR-He in meteoroid fragments must be present in the seafloor He inventory.

The ^{3}He content of 75 individual 0.05–50 ng stratospheric IDPs (equivalent to 4–40 µm diameter spheres of 2 g/cc) varies by approximately two orders of magnitude (0.07–26 × 10^6 atoms; Nier and Schlutter, 1990, 1992; Pepin et al., 2000, 2001), but is independent of particle mass (Fig. 3). This range is indistinguishable from that measured in 5–10 mg samples of VA13/2 (Fig. 3) and to a first order the ^{3}He in the VA13/2 samples could be derived from a small number of whole IDPs. The mean IDP ^{3}He content (1.3 ± 3.2 × 10^6 atoms) is indistinguishable from the VA13/2 sample average (1.3 ± 5.7 × 10^6 atoms; $n = 16$). The average ^{3}He content of unphosphatized CD29-2 samples (2.0 ± 6.8 × 10^5 atoms; $n = 15$) is significantly lower than whole IDP ^{3}He content and cannot easily be derived from the 7–20 µm IDPs that dominate the He inventory of oceanic sediments (Farley et al., 1997).

To quantify the likelihood that the crust ^{3}He distributions can be derived from the IDP population we use the Kolmorov–Smirnov (K-S) test (http://www.physics.csbsju.edu/stats/KS-test.n.plot_form.html) to compare whether the crust datasets differ significantly from the IDP population. In these tests the null hypothesis is that both datasets are similar. For CD29-2 the maximum difference between cumulative distributions (D) is 0.5467 with a corresponding P value of 0.001. The two datasets are statistically different at the 95% confidence level and consequently it is difficult to derive the CD29-2 ^{3}He distribution from the single 4–40 µm IDP population.
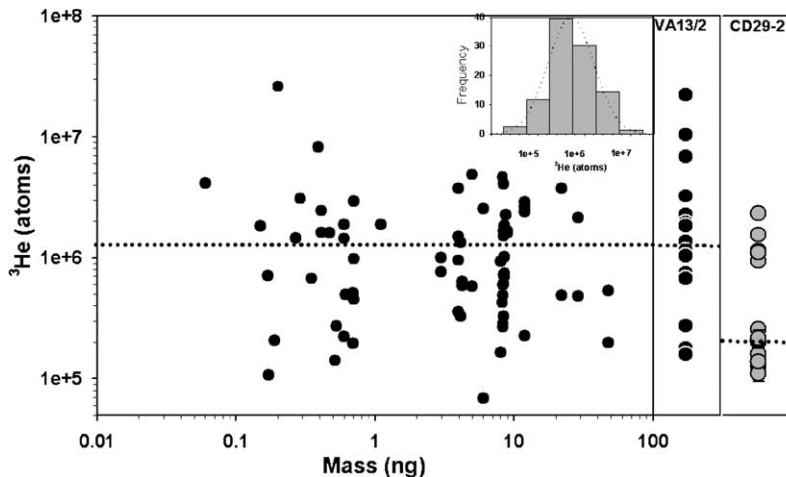
Fig. 3. Plot of ^{3}He content vs. mass for 75 individual or cluster IDPs sampled in the stratosphere (Nier and Schlutter, 1990, 1992; Pepin et al., 2000, 2001). The ^{3}He content is independent of IDP mass and the distribution is log normal, with a geometric mean value of 1.3×10^6 atoms indicated by dotted line. The ^{3}He in VA13/2 and unphosphatized CD29-2 samples, and their means, are shown for comparison. For discussion see text.

Applying the KS-test to the VA13/2 data yields a D value of 0.1608 with a corresponding P value of 0.853. This implies that the two datasets are not significantly different and, therefore, it is possible to generate the VA13/2 ^{3}He concentrations from the IDP population. However, if the VA13/2 He concentration distribution is the product of a very small number of IDPs, natural variation in particle number would leave some samples with no particles, and therefore no ^{3}He$_{et}$. This never occurs (Table 1). A quantitative estimate of the number of particles can be made from the absolute value of the difference in He concentration between replicate analyses of the same sample. This fractional difference (FD) is determined from

$$FD = (a - b)/(a + b)/2, \qquad (2)$$

where a is the He concentration in one sub-sample and b represents the He in the other replicates. In Fig. 4, we show how the fractional difference between pairs varies depending on the difference in the number of particles between replicates if the particles have comparable He concentration. We have determined He isotopes in 4 homogenised aliquots from samples VA13/2(0-1) and VA13/2(5-6) (Table 1). The 12 fractional differences are plotted in Fig. 5. Peaks at low (0–0.2) and high values (1.6–1.8) appear in the dataset with few intermediate values. If all particles have the same He content, the extremely low FD of the samples can only be produced by small variations in large numbers of particles, with the lowest values providing a constraint on the number of particles. Values at 0.05 put a lower limit on the particle number of 20. This is supported by the presence of high FD values which cannot be produced by small numbers of particles in each aliquot without one having zero particles (Fig. 4). High values require large differences in particle number between each
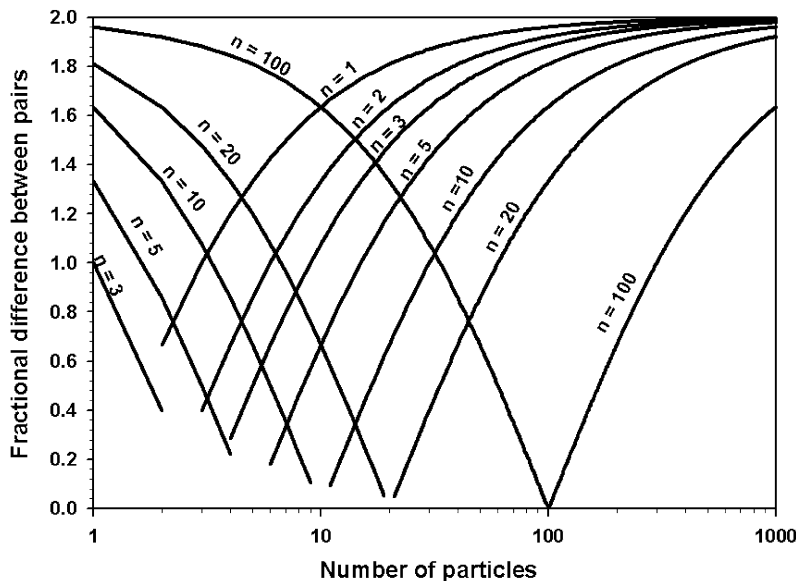

Fig. 4. The fractional differences between replicate pairs for variable number of particles (1–1000). The number of particles trapped by the first sub-sample is denoted by n, and the corresponding curves represent the changes in fractional difference depending on number of particles in replicates.
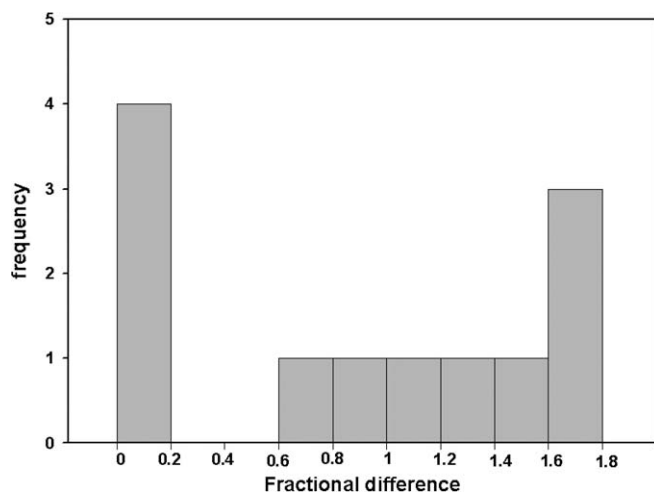
Fig. 5. The fractional differences between 12 pairs of replicated analyses for VA13/2(0-1) and VA13/2(5-6). Values vary between 0 and 1.8, with most of the data lying in the interval 0 to 0.2, and 1.6 to 1.8 with few intermediate values.

pair. For instance, a fractional difference of 1.8 (these make up 25% of the data) between two sub-samples requires 20 and 1, or 20 and 400 particles. Values of 1.4 for a given pair of replicates can be generated by 10 and 2, or 10 and 55 particles/sample. Such variations are unlikely to be frequently sampled by normal distributions.

The simplest explanation for these observations is that a large number of relatively He-poor particles carry much of the ^{3}He in VA13/2, but that frequently small numbers of extremely He-rich particles are present that dominate the inventory. The high ^{3}He/^{4}He of the ^{3}He-rich sub-samples (e.g. VA13/2(0-1)b, (0-1)d and (5-6)a) implies that the He in the rare particles is dominantly galactic cosmic ray in origin. The He-poor particles may be μm-sized grains of magnetite and silicates that remain after weathering of the IDPs on the seafloor, or more robust partially melted micrometeorites that are known to contain significant He_{et} (e.g. Stuart et al., 1999).

The distribution of FD from VA13/2 bears little similarity to the admittedly larger dataset from oceanic sediments. In sediment samples from the Ontong Java Plateau over 85% of pairs have fractional differences of less than 0.5, with only 3% having values in excess of 1 (Farley et al., 1997). This difference may reflect the small crust dataset and clearly more work is required in order to demonstrate it more convincingly. However, it is consistent with the evidence presented previously (see Section 4.2) for the preferential incorporation of large, dense dust particles by the crusts.

4.4. Helium isotope variation in CD29-2: the effect of phosphatization

^{4}He concentrations in CD29-2 show a marked decrease at around 52 mm (ca. 42 Ma). From a maximum of over 10^{14} atoms/g, the range measured in the CD29-2 samples younger than 42 Ma (0.4–6.7×10^{12} atoms/g) is up to 350 times lower (Table 1, Fig. 2a). Although the higher ^{4}He

concentration in the 42 Ma and older samples could be due to a change in the crustal radiogenic He delivered in detrital grains, the absence of a relationship between ^{4}He and Si (Fig. 6a) provides no support for an origin in continental dust. The ^{4}He enrichment coincides with the impregnation of CFA into the crust between 52 mm and the base of the crust. The phosphatization took place by the replacement of calcite microfossils that filled pore space by CFA, the replacement of primary Fe oxyhydroxide by CFA and direct precipitation into pore spaces (Hein et al., 2000). The link between ^{4}He and crust alteration is supported by a broad correlation between ^{4}He and P in the phosphatized section of the crust (Fig. 6b). For example, all but one of the 10 samples with the highest P have the highest ^{4}He concentrations. Phosphatization results in a slight depletion of U (Hein et al., 2000). Consequently, the high He cannot be due to increased ^{4}He production. It is more likely that the high ^{4}He concentration reflects better retention of *in situ* radiogenic helium due to the increase in grain size and decrease in porosity that results from phosphatization. For
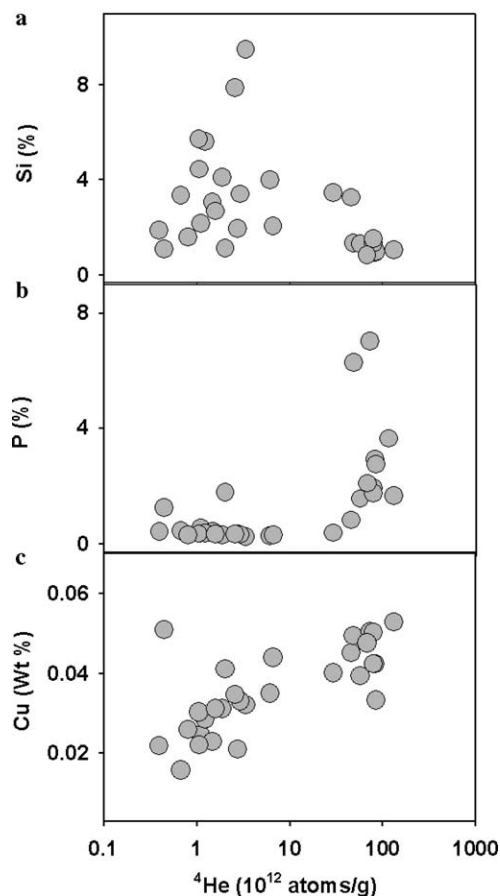

Fig. 6. (a) ^{4}He vs. Si content in CD29-2. The absence of a correlation indicates that variation in ^{4}He is not controlled by the detrital mineral contribution. (b) The positive correlation between ^{4}He and P in CD29-2 indicates that the phosphatized crust retains *in situ* ^{4}He better than unaltered crust. (c) This is supported by ^{4}He co-variation with Cu. The high Cu content of the altered crust is due to incorporation of Cu during reducing conditions.

an average U concentration of 6 ppm, even the maximum ^{4}He in the altered layers (CD29-2 (61-62)) requires the retention of only 12% of the total radiogenic He produced *in situ*. Phosphatization occurs under suboxic and reducing environment related to an extensive oxygen-minimum zone. This results in increased input of nutrient-type elements such as Cu that may be related to a non-CFA biogenic phase (Koschinsky et al., 1997). The correlation of ^{4}He with Cu indicates that He retention is strongest in the phosphatized crust (Fig. 6c).

Unlike ^{4}He, there is no pronounced change of ^{3}He concentrations at 52 mm. ^{3}He concentrations show a marked decrease in crust that is older than 56 Ma (from 87 to 105 mm) (Fig. 2b). The 8 samples that are older than 63 Ma have an average of 0.3×10^7 atoms ^{3}He/g (assuming (12-13B), (2-3B), and (0-1B) have ^{3}He at detection limit). This is six times lower than the average concentration of the younger layers. There is no systematic variation of ^{3}He concentrations in the layers of young crust that might indicate a continuous process, such as diffusion, was responsible for ^{3}He loss from the extraterrestrial grains with time. In fact, it has been seen that extraterrestrial ^{3}He is unambiguously well preserved in sediments up to 70 Ma from GPC-3, close to crust sampling sites (Farley, 1995). The low ^{3}He concentration in the old crust may be due to (i) a lower flux of extraterrestrial particles, (ii) less efficient trapping of extraterrestrial grains, (iii) lower ^{3}He content of extraterrestrial grains, or (iv) the breakdown of the extraterrestrial particles during diagenesis. The first three options are clearly difficult to test. The last possibility is likely and consistent with earlier studies that have shown how trapped noble gas concentrations are lost from Antarctic MMs during alteration on Earth surface (Osawa et al., 2003). Diagenetic breakdown of IDPs and MMs, and concomitant loss of extraterrestrial He (and Ne), is another nail in the coffin for the proposition that the subduction of extraterrestrial dust in oceanic sediments is the source of primordial noble gas reservoir in the deep Earth (Anderson, 1993).

5. Conclusions

Helium isotopes in samples of two ferromanganese crusts (VA13/2 and CD29-2) from the central Pacific Ocean are dominantly a mixture of solar implanted He, hosted by extraterrestrial grains, and radiogenic He in wind-borne dust. *In situ* ^{4}He concentrations never exceed 12% of the theoretical minimum amount produced by U and Th decay, probably as a result of recoil and diffusion. In most samples ^{4}He concentrations are remarkably constant and variation in ^{3}He/^{4}He reflects the variation in the extraterrestrial He contribution. The ^{3}He/^{4}He of crust VA13/2 require a contribution from galactic cosmic ray-derived He in at least two samples. Helium concentrations are orders of magnitude lower than in oceanic sediments reflecting the low trapping efficiency of in-falling terrestrial and extraterrestrial grains by Fe-Mn crusts. The low

extraterrestrial ^{3}He concentration of the crusts rule out whole 4–40 μm IDPs as the source and implies that refractory grains from smaller IDPs and/or partially degassed micrometeorites are the dominant source. Higher ^{4}He, and lower ^{3}He concentrations in samples older than 45 Ma in crust CD29-2 are correlated with phosphatization. The data are explained by better retention of *in situ*-produced ^{4}He and loss of extraterrestrial ^{3}He due to grain breakdown.

References

Amari, S., Ozima, M., 1988. Extraterrestrial noble gases in deep-sea sediments. *Geochim. Cosmochim. Acta* **52**, 1087–1095.

Anderson, D.L., 1993. Helium-3 from the mantle: primordial signal or cosmic dust? *Science* **261**, 170–176.

Benkert, J.P., Baur, H., Signer, P., Wieler, R., 1993. He, Ne, Ar from the solar wind and solar energetic particles in lunar ilmenites and pyroxenes. *J. Geophys. Res.* **98**, 13147–13162.

Burton, K.W., Bourdon, B., Birck, J., Allègre, C.J., Hein, J.R., 1999. Osmium isotope variations in the oceans recorded by Fe-Mn crusts. *Earth Planet. Sci. Lett.* **171**, 185–197.

Busemann, H., Baur, H., Wieler, R., 1998. Light noble gases in phase Q of Cold Bokkeveld (CM2): Neon-E and a new 3He/4He in Q close to Helium-A. *Meteorit. Planet. Sci.* **33**, A28, abstr.

Christensen, J.N., Halliday, A.N., Godfrey, L.V., Hein, J.R., Rea, D.K., 1997. Climate and ocean dynamics and the lead isotopic records in Pacific ferromanganese crusts. *Science* **277**, 913–918.

Esser, B.K., Turekian, K.K., 1988. Accretion rate of extraterrestrial particles determined from osmium isotope systematics of Pacific pelagic clay and manganese nodules. *Geochim. Cosmochim. Acta* **52**, 1383–1388.

Farley, K.A., 1995. Cenozoic variations in the flux of interplanetary dust recorded by ^{3}He in a deep sea sediment. *Nature* **376**, 153–156.

Farley, K.A., 2000. Helium diffusion from apatite: general behaviour as illustrated by Durango fluorapatite. *J. Geophys. Res.* **105**, 2903–2914.

Farley, K.A., 2001. Extraterrestrial helium in seafloor sediments: identification, characteristics and accretion rate over time. In: Peucker-Ehrenbrink, B., Schmitz, B. (Eds.), *Accretion of Extraterrestrial Matter Throughout Earth's History*. Kluwer, New York, pp. 179–204.

Farley, K.A., Wolf, R.A., Silver, L.T., 1996. The effects of long alpha-stopping distances on U-Th/He ages. *Geochim. Cosmochim. Acta* **60**, 4223–4229.

Farley, K.A., Love, S., Patterson, D.B., 1997. Atmospheric entry heating and helium retentivity of interplanetary dust particles. *Geochim. Cosmochim. Acta* **61**, 2309–2317.

Farley, K.A., Montanari, A., Shoemaker, E.M., Shoemaker, C.S., 1998. Geochemical evidence for a comet shower in the late eocene. *Science* **280**, 1250–1253.

Frank, M., 2002. Radiogenic isotopes: tracers of past ocean circulation and erosional input. *Rev. Geophys.* **40**. doi:10.1029/2000RG000094.

Frank, M., O'Nions, R.K., Hein, J.R., Banaker, V.K., 1999. 60 Ma record of major elements and Pb-Nd isotopes from hydrogeneous ferroman-

ganese crusts: Reconstruction of seawater. Paleochemistry. *Geochim. Cosmochim. Acta* **63**, 1689–1708.

Friedrich, G., Schmitz-Wiechowsky, A., 1980. Mineralogy and chemistry of a ferromanganese crust from a deep-sea hill, central Pacific, "Valdivia" cruise VA 13/2. *Mar. Geol.* **37**, 71–90.

Fukumoto, H., Nagao, K., Matsuda, J., 1986. Noble gas studies on the host phase of high ^{3}He/^{4}He ratios in deep sea sediment. *Geochim. Cosmochim. Acta* **50**, 2245–2253.

Geiss, J., Buehler, F., Cerutti, H., Eberhardt, P., Filleaux, C.H., 1972. Solar wind composition experiments. *Apollo 16 Prel. Sc. Ret.* NASA SP-315, 14.1–14.10.

Halbach, P., Segl, M., Puteanus, D., Mangini, A., 1983. Co fluxes and growth rates in ferromanganese deposits from central Pacific seamount areas. *Nature* **304**, 719–722.

Hein, J.R., Morgan, C.L., 1999. Influence of substrate rocks on Fe-Mn crust composition. *Deep Sea Res. I* **46**, 855–875.

Hein, J.R., Manheim, F.T., Schwab, W.C., Davis, A.S., 1985. Ferromanganese crusts from Necker Ridge, Horizon Guyot, and S.P. Guyot: geological considerations. *Mar. Geol.* **69**, 25–54.

Hein J.R., Kirschenbaum H., Schwab W.C., Usui A., Taggart J.E., Stewart K.C., Davis A.S., Terashima S., Quinterno P.J., Olson R.L., Pickthorn L.G., Schulz M.S., Morgan C.L., 1990. Mineralogy and geochemistry of Co-rich ferromanganese crusts and substrate rocks from Karin Ridge and Johnston Island, Farnella Cruise F7-86-HW.U.S. Geological Survey Open File Report 90-298, 80 pp.

Hein, J.R., Koschinsky, A., Bau, M., Manheim, F.T., Kang, J., Roberts, L., 2000. Cobalt-rich ferromanganese crusts in the Pacific. In: Cronan, D.S. (Ed.), *Handbook of Marine Mineral Deposits.* CRC Press, Boca Raton, FL, pp. 239–279.

Henderson, G.M., Burton, K.W., 1999. Using ^{234}U/^{238}U to assess diffusion rates of isotope tracers in ferromanganese crusts. *Earth Planet. Sci. Lett.* **170**, 169–179.

Klemm, V., Levasseur, S., Frank, M., Hein, J.R., Halliday, A.N., 2005. Osmium isotope stratigraphy of a marine ferromanganese crust. *Earth Planet. Sci. Lett.* **238**, 42–48.

Knie, K., Korchinek, G., Faestermann, T., Dorfi, E.A., Rugel, G., Wallner, A., 2004. ^{60}Fe anomaly in a deep-Sea Manganese Crust for a nearby supernova source. *Phys. Rev. Lett.* **93**, 9. doi:10.1103/PhysRevLett.93.171103.

Koschinsky, A., Stascheit, A., Bau, M., Halbach, P., 1997. Effects of phosphatization on the geochemical and mineralogical composition of marine ferromanganese crusts. *Geochim. Cosmochim. Acta* **61**, 4079–4094.

Lal, D., Jull, A., 2005. On the fluxes and fates of ^{3}He accreted by the earth with extraterrestrial particles. *Earth Planet. Sci. Lett.* **235**, 375–390.

Ling, H.F., Burton, K.W., O'Nions, R.K., Kamber, B.S., von von Blanckenburg, F., Gibb, A.J., Hein, J.R., 1997. Evolution of Nd and Pb isotopes in Central Pacific seawater from ferromanganese crusts. *Earth Planet. Sci. Lett.* **146**, 1–12.

Lupton, J.E., Klinkhammer, G.P., Normark, W.R., Haymon, R., Macdonald, K.C., Weiss, R.F., Craig, H., 1980. Helium-3 and manganese at the 21°N East Pacific Rise hydrothermal site. *Earth Planet. Sci. Lett.* **50**, 115–127.

Marcantonio, F., Anderson, R.F., Stute, M., Kumar, N., Schlosser, P., Mix, P., 1996. Extraterrestrial ^{3}He as a tracer of marine sediment and transport. *Nature* **383**, 705–707.

Marty, B., Robert, P., Zimmermann, L., 2005. Nitrogen and noble gases in micrometeorites. *Meteorit. Planet. Sci.* **40**, 881–894.

Matsuda, J., Murota, M., Nagao, K., 1990. He and Ne isotopic studies on the extraterrestrial material in deep sea sediments. *J. Geophys. Res.* **95**, 7111–7117.

Mukhopadhyay, S., Farley, K.A., Montanari, A., 2001. A 35 Myr record of helium in pelagic limestones from Italy: implications for interplanetary dust accretion from the early Maastrichtian to the middle Eocene. *Geochim. Cosmochim. Acta* **65**, 653–669.

Nier, A.O., Schlutter, D.J., 1990. Helium and neon isotopes in stratospheric dust particles. *Meteoritics* **25**, 263–267.

Nier, A.O., Schlutter, D.J., 1992. Extraction of helium from individual interplanetary dust particles by step-heating. *Meteoritics* **27**, 166–173.

Osawa, T., Nagao, K., 2002. Noble gas composition of Antarctic micrometeorites collected at the Dome Fuji Station in 1996 and 1997. *Meteorit. Planet. Sci.* **37**, 911–936.

Osawa, T., Nakamura, T., Nagao, K., 2003. Noble gas isotopes and mineral assemblages of Antarctic micrometeorites collected at the meteorite ice field around the Yamato mountains. *Meteorit. Planet. Sci.* **38**, 1627–1640.

Ozima, M., Takayanagi, M., Zashu, S., Amari, S., 1984. High ^{3}He/^{4}He in ocean sediments. *Nature* **311**, 449–451.

Patterson, D.B., Farley, K.A., 1998. Extraterrestrial ^{3}He in seafloor sediments: evidence for correlated 100 kyr periodicity in the accretion rate of interplanetary dust, orbital parameters, and Quaternary climate. *Geochim. Cosmochim. Acta* **62**, 3669–3682.

Patterson, D.B., Farley, K.A., Norman, M.D., 1999. ^{4}He as a tracer of continental dust: a 1.9 million year record of aeolian flux to the west equatorial Pacific Ocean. *Geochim. Cosmochim. Acta* **63**, 615–625.

Pepin, R.O., Palma, R.L., Schlutter, D.J., 2000. Noble gases in interplanetary dust particles. I. The excess of helium-3 problem and estimates of the relative fluxes of solar wind and solar energetic particles in interplanetary space. *Meteorit. Planet. Sci.* **35**, 495–504.

Pepin, R.O., Palma, R.L., Schlutter, D.J., 2001. Noble gases in interplanetary dust particles. II: excess helium-3 in cluster particles and modelling constraints on interplanetary dust particles exposures to cosmic ray irradiation. *Meteorit. Planet. Sci.* **36**, 1515–1534.

Peucker-Ehrenbrink, B., 1996. Accretion of extraterrestrial matter during the last 80 million years and its effect on the marine osmium record. *Meteorit. Planet. Sci.* **60**, 3187–3196.

Sano, Y., Toyoda, K., Wakita, H., 1985. ^{3}He/^{4}He ratios of marine ferromanganese nodules. *Nature* **317**, 518–520.

Segl, M., Mangini, A., Bonani, G., Hofmann, H., Nessi, M., Suter, M., Wolfli, W., Friedrich, G., Pliger, W., Wiechowski, A., Beer, J., 1984. Be dating of manganese crust from Central North Pacific and implications for oceanic palaeocirculation. *Nature* **309**, 540–543.

Shuster, D.L., Vasconcelos, P.M., Heim, J.A., Farley, K.A., 2005. Weathering geochronology by (U-Th)/He dating of goethite model. *Geochim. Cosmochim. Acta* **69**, 659–673.

Stuart, F.M., Turner, G., Taylor, R.P., 1994. He-Ar isotope systematics of fluid inclusions: resolving mantle and crustal contributions to hydrothermal fluids. In: *Noble Gas Geochemistry and Cosmochemistry.* Terra Sci Publ., pp. 261–278.

Stuart, F.M., Harrop, P.J., Knott, S., Turner, G., 1999. Laser extraction of helium isotopes from Antarctic micrometeorites: source of He and implications for the flux of extraterrestrial ^{3}He to earth. *Geochim. Cosmochim. Acta* **17**, 2653–2665.

Takayanagi, M., Ozima, M., 1987. Temporal variation of ^{3}He/^{4}He ratio recorded in deep sea sediment cores. *J. Geophys. Res.* **92**, 12531–12538.

Trull, T.W., Kurz, M.D., Jenkins, W.J., 1989. Diffusion of cosmogenic ^{3}He in olivine and quartz: implications for surface exposure dating. *Earth Planet. Sci. Lett.* **103**, 241–256.

Turner, G., Stuart, F.M., 1992. He/heat ratios and the deposition temperatures of ocean-floor sulfides. *Nature* **357**, 581–583.

Van de Flierdt, T., Frank, M., Halliday, A.N., Hein, J.R., Hattendorf, B., Gunther, D., Kubik, P.W., 2003. Lead isotopes in North Pacific deep water – implications for past changes in input sources and circulation patterns. *Earth Planet. Sci. Lett.* **209**, 149–164.

Von Stackelberg, U., Kunzendorf, H., Marchig, V., Gwozdz, R., 1984. Growth history of a large ferromanganese crust from the equatorial north Pacific nodule belt. *Geol. Jahrb.* **A75**, 213.

Weiler, R., 2002. Cosmic-ray-produced noble gases in meteorites. In: Porcelli, D., Ballentine, C.J., Weiler, R. (Eds.), *Noble Gases in Geochemistry and Cosmochemistry.* The Mineralogical Society of America, Washington, DC, pp. 125–170.

Wernicke, R.S., Lippolt, H.J., 1994. ^{4}He age discordance and release behaviour of a double shell botryoidal haematite from Schwarzwald, Germany. *Geochim. Cosmochim. Acta* **58**, 421–429.

Winckler, G., Anderson, R.F., Stute, M., Schlosser, P., 2004. Does interplanetary dust control 100 kyr glacial cycles? *Quat. Sci. Rev.* **23**, 1873–1878.

Yamazaki, T., Tomishima, Y., Handa, K., Tsurusaki, K., 1990. Fundamental study on remote sensing of engineering properties of cobalt rich manganese crusts. In: Salama, M.M., Rhee, H.C., Williams, J.G., Liu, S. (Eds.), *Proceedings, Ninth International Conference of Offshore Mechanics and Arctic Engineers*. The American Society of Mechanical Engineers Book No. 10296E, pp. 605–610.